ELSEVIER

Nuclear Physics B 501 [FS] (1997) 773–799

NUCLEAR PHYSICS B

Analytic calculation of conformal partition functions: Tricritical hard squares with fixed boundaries

David L. O'Brien, Paul A. Pearce, S. Ole Warnaar

Department of Mathematics, The University of Melbourne, Parkville, Victoria 3052, Australia

Received 3 January 1997; revised 11 April 1997; accepted 19 June 1997

Abstract

An analytic method of calculating conformal partition functions of solvable lattice models is presented. Our technique involves the solution of transfer matrix functional equations in the scaling limit, and unifies the work of Albertini et al. on the classification of transfer matrix eigenvalues with that of Klümper and Pearce on finite-size corrections. As an illustration, conformal partition functions of the tricritical hard square model with fixed boundaries are derived. The resulting Virasoro characters arise in their fermionic representation and agree with the Coulomb gas calculations of Saleur and Bauer. © 1997 Elsevier Science B.V.

PACS: 75.10.Hk; 11.25.Hf; 05.70.Jk

Keywords: Conformal partition functions; Hard square model; Fixed boundaries; Virasoro characters

1. Introduction

Solvable lattice models have long proven to be valuable tools in the study of critical phenomena. Since the advent of conformal invariance in particular [1,2], many theoretical predictions have been confirmed by direct analytic calculations on solvable models. Indeed, techniques to calculate such quantities as central charges and conformal weights have now become standard [3–10]. However, confirmation of the predictions of conformal invariance regarding conformal partition functions[1] is a rather more difficult problem, and fully analytic derivations have so far been restricted to the Ising model [11,12].

[1] Following Ref. [17], we refer to the universal part of the partition function as the "conformal" partition function.

PII S0550-3213(97)00424-0

There are two ingredients necessary for an analytic calculation of conformal partition functions from solvable lattice models: the complete classification of all eigenvalues of the row-to-row transfer matrix in the leading band; and the exact calculation of finite-size corrections to each of these eigenvalues. Important steps towards such a calculation have been taken in the work of the Stony Brook group [13–17] and the work of Klümper and Pearce [8–10]. The former work, performed in the context of the three-state Potts model, provided a general approach to the classification of all transfer matrix eigenvalues. Although this led to the computation of conformal partition functions, the finite-size corrections to the eigenvalues in the leading band were determined numerically [17]. In contrast, in the latter work an approach was developed for the analytic derivation of such finite-size corrections, but only for the primary scaling dimensions.

In this paper we present an analytic technique for computing conformal partition functions of solvable lattice models. Specifically, we follow the methods of Albertini et al. [13] for the classification of transfer matrix eigenvalues. We then extend the methods of Klümper and Pearce [9] to calculate analytically the finite-size corrections to all eigenvalues in the leading band.

To demonstrate our method we derive conformal partition functions for the tricritical hard square model with fixed boundaries, thus confirming the predictions of Saleur and Bauer [18] based on Coulomb gas calculations [19–21]. The model has been chosen as the simplest non-free-fermion model, whilst the fixed boundaries have been chosen to give the simplest possible classification of the leading band of eigenvalues.

This paper is organized as follows. In the next section we introduce Baxter's tricritical hard square model with fixed boundaries, and give a functional equation satisfied by the row transfer matrix. In Section 3 we define the conformal partition function for cylindrical geometries. Sections 4 to 9 are devoted to solving the functional equation to obtain the conformal partition functions. These six sections correspond to the independent choices of boundary, and each yields one of the six $c = \frac{7}{10}$ Virasoro characters in its fermionic representation [16]. We conclude with a brief discussion.

2. The tricritical hard square model

Baxter's hard square model is a gas of interacting hard-core particles on the two-dimensional square lattice [22–24]. Each site of the lattice carries a spin μ which can take the value 0 or 1. Spins on adjacent sites must satisfy $\mu\mu' = 0$, so that allowed spin configurations correspond to configurations of hard-core square particles rotated by 45° with respect to the lattice. Adjacent particles interact, with partition function

$$\Xi(L, M, z) = \sum_{\substack{\text{particle} \\ \text{configurations}}} z^N \mathrm{e}^{LN_1 + MN_2}, \tag{2.1}$$

where N is the number of particles, N_1 the number of adjacent particles in the NE–SW direction, and N_2 the number of adjacent particles in the NW–SE direction. Baxter has shown the model to be integrable on the manifold $z = (1 - \mathrm{e}^{-L})(1 - \mathrm{e}^{-M})/$

$(e^{L+M} - e^{L} - e^{M})$. The phase diagram of the hard square model has been discussed by Huse [25], who showed that on a particular line of the solvable manifold the model becomes tricritical.

A convenient reformulation of the model is given by the four-state Andrews–Baxter–Forrester model [26]. In this representation, sites of the square lattice take heights from the set $\{1,2,3,4\}$ subject to the condition that the values of heights on adjacent sites must differ by ± 1. When the heights 1 and 4 are identified with $\mu = 1$ and the heights 2 and 3 with $\mu = 0$, the allowed lattice configurations reproduce the hard square model. The Boltzmann weights of the tricritical hard square model in the ABF formulation are

$$W\begin{pmatrix} d & c \\ a & b \end{pmatrix} = \frac{\sin(\lambda - u)}{\sin\lambda}\,\delta_{a,c} + \frac{\sin u}{\sin\lambda}\left(\frac{S_a S_c}{S_b S_d}\right)^{1/2}\delta_{b,d}, \tag{2.2}$$

where $\lambda = \frac{1}{5}\pi$ and $S_a = \sin(a\lambda)$. The parameter u lies in the range $0 < u < \lambda$, with the point $u = \frac{1}{2}\lambda$ corresponding to $L = M$.

Since the weights satisfy the Yang–Baxter equation [23], they ensure commuting transfer matrices on a periodic lattice. On a lattice with boundaries it is necessary to introduce left and right boundary weights which satisfy reflection equations [27,28]. Such weights have been obtained in Ref. [29], and for our purposes we select

$$K\begin{pmatrix} a & \\ a & a \pm 1 \end{pmatrix} = \left(\frac{S_{a\pm 1}}{S_a}\right)^{1/2} \frac{\sin(\lambda - u \pm \xi)\sin(\lambda - u \mp a\lambda \mp \xi)}{\sin^2\lambda},$$

$$K\begin{pmatrix} a \pm 1 & a \\ & a \end{pmatrix} = \left(\frac{S_{a\pm 1}}{S_a}\right)^{1/2}. \tag{2.3}$$

The parameter ξ is restricted to the range $\frac{1}{2}\lambda < \xi < \lambda$, but is otherwise arbitrary.

We use the face and boundary weights to construct a (double-row) transfer matrix $\boldsymbol{T}$ [29]. For a lattice of width N, the entry of $\boldsymbol{T}$ corresponding to rows of heights $\boldsymbol{a} = \{a_1, \ldots, a_{N-1}\}$ and $\boldsymbol{b} = \{b_1, \ldots, b_{N-1}\}$ is defined diagrammatically by

$\boldsymbol{T}(u)_{\boldsymbol{a},\boldsymbol{b}} = \sum_{c_0,\ldots,c_N}$

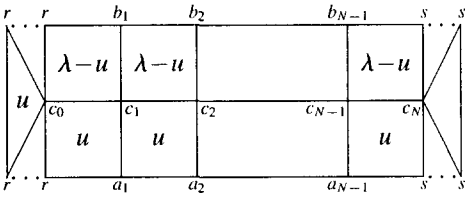

, (2.4)

where the triangles and squares represent the boundary and face weights respectively. The adjacency condition on the heights of the model can be encoded in the 4×4 incidence matrix A with entries $A_{j,k} = \delta_{|j-k|,1}$. The dimension of $\boldsymbol{T}$ is then simply expressed in terms of A^N as

$$\dim \boldsymbol{T} = A^N_{r,s}. \tag{2.5}$$

In Ref. [29], a functional equation for $\boldsymbol{T}(u)$ has been obtained. By defining a normalized transfer matrix

$$\boldsymbol{t}(u) = (-1)^s \alpha_r(u - \xi)\,\alpha_{-r}(u + \xi)\,\beta(u)\,\gamma_2(u)\,\boldsymbol{T}(u)/\gamma_1(u)\,\gamma_3(u) \tag{2.6}$$

this equation takes the simple form

$$t(u)\,t(u+\lambda) = I + t(u+3\lambda). \tag{2.7}$$

In this normalization we have used the definitions

$$\gamma_k(u) = (-1)^N \left(\frac{\sin(u+k\lambda)}{\sin\lambda}\right)^{2N}, \qquad \beta(u) = \frac{\sin^2(2u-\lambda)}{\sin(2u-3\lambda)\sin(2u+\lambda)},$$
$$\alpha_a(u) = \frac{\sin\lambda\sin(u+(3-a)\lambda)\sin(u+(1-a)\lambda)}{\sin u\sin(u-\lambda)\sin(u+2\lambda)}. \tag{2.8}$$

The arbitrary factor of $(-1)^s$ in Eq. (2.6) has been included so that Eq. (2.7) takes a form independent of s.

Before we actually solve the functional equation (2.7) in later sections, let us note one property of the eigenvalues of t which follows directly from the weights (2.2) and (2.3). Using these weights it follows that

$$\lim_{iu\to\infty} \sum_g e^{-4iu} \quad \begin{array}{ccccc} a & \cdots & a & & d \\ & u & & \lambda-u & \\ & & g & & c \\ & & & u & \\ a & \cdots & a & & b \end{array} \quad = \lim_{iu\to\infty} \rho e^{-2iu} \quad \begin{array}{ccc} d & & \\ & u & c \\ b & & \end{array} \quad \delta_{b,d}, \tag{2.9}$$

with $\rho^{-1} = -4\exp(i\lambda)\sin^2\lambda$, and we conclude that $t(u)$ is diagonal in the limit $iu \to \infty$. If we N times apply (2.9) to the transfer matrix and then use

$$\lim_{iu\to\infty} \sum_g e^{-2iu} \quad \begin{array}{ccc} a & & a \\ & u & \\ & g & \\ a & & a \end{array} \quad = -2\rho\cos(a\lambda), \tag{2.10}$$

we find

$$\lim_{iu\to\infty} t(u)_{a,a} = \lim_{iu\to\infty} \frac{(-1)^{s+1}}{(\rho e^{2iu})^{N+1}} T(u)_{a,a} = (-1)^{s+1} 2\cos(s\lambda), \tag{2.11}$$

independent of a. The fact that only the two values $2\cos\lambda = \frac{1}{2}(1+\sqrt{5})$ and $2\cos(3\lambda) = \frac{1}{2}(1-\sqrt{5})$ occur can be understood by taking the limit $iu \to \infty$ in the functional equation (2.7). We will need the result (2.11) in Sections 4 to 9.

3. Conformal properties of the tricritical hard square model

We here briefly recall some of the properties of the tricritical hard square model with fixed boundaries as predicted by conformal invariance. Consider the finite-size partition function Z_{NM} of the tricritical hard square model on a cylindrical lattice of width N and

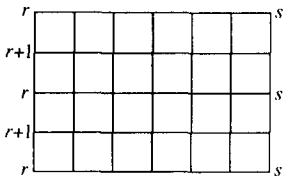

Fig. 1. Fixed boundaries on the square lattice. Unlabelled sites are free.

Table 1
Grid of conformal weights $\Delta_{r,s} = \frac{1}{80}[(5r-4s)^2 - 1]$ for the unitary minimal theory with $c = \frac{7}{10}$.

s \ r	1	2	3
4	3/2	7/16	0
3	3/5	3/80	1/10
2	1/10	3/80	3/5
1	0	7/16	3/2

circumference M. The asymptotic behaviour of Z_{NM} in the limit of large N and M with the ratio M/N fixed is given by

$$Z_{NM}(u) = \mathrm{Tr}\big(\boldsymbol{T}(u)^M\big) \sim \exp\big(-NMf_{\mathrm{b}}(u) - Mf_{\mathrm{s}}(u)\big)\, Z(q). \tag{3.1}$$

Here $\boldsymbol{T}$ is the row transfer matrix, f_{b} is the bulk free energy, f_{s} is the surface free energy, and $Z(q)$ is the universal conformal partition function with modular parameter

$$q = \exp(-2\pi \sin(5u)\, M/N). \tag{3.2}$$

To leading orders, each transfer matrix eigenvalue $T(u)$ reads [30]

$$\ln T(u) = -Nf_{\mathrm{b}}(u) - f_{\mathrm{s}}(u) + \frac{2\pi}{N}\left(\tfrac{1}{24}c - \Delta - n\right)\sin(5u) + \mathrm{o}\left(\frac{1}{N}\right), \tag{3.3}$$

where $c = \frac{7}{10}$ is the central charge, Δ is one of the conformal weights in Table 1, and n is a non-negative integer which is zero for the largest eigenvalue. After taking the ratio of each eigenvalue with the largest, we can write

$$Z(q) = \sum_{k=1}^{3}\sum_{l=1}^{2} q^{-\frac{c}{24}+\Delta_{k,l}} \mathcal{N}(\Delta_{k,l}) \sum_{j} q^{n_j} = \sum_{k=1}^{3}\sum_{l=1}^{2} \mathcal{N}(\Delta_{k,l})\, \chi_{k,l}(q), \tag{3.4}$$

with $\mathcal{N}(\Delta_{k,l}) = 0$ or 1 and $\chi_{k,l}$ one of the $c = \frac{7}{10}$ Virasoro characters.

The operator content $\mathcal{N}(\Delta_{k,l})$ is determined by the particular choice of boundary conditions on the cylinder [31,18]. For a lattice with the boundary conditions (r,s) depicted in Fig. 1, Saleur and Bauer [18] have used Coulomb gas techniques to calculate $\mathcal{N}(\Delta_{k,l}) = \delta_{k,r}\delta_{l,s}$, so the conformal partition function is given by

$$Z(q) = \chi_{r,s}(q). \tag{3.5}$$

Returning to the transfer matrix defined in Eq. (2.4), observe that we have chosen our boundary weights (2.3) to correspond to the lattice in Fig. 1. Every second site on

the right boundary is fixed to the same height s, and the remaining right boundary sites are freely summed over. Furthermore, at the point $u = \lambda - \xi$ we have

$$K\begin{pmatrix} r & r+1 \\ r & \end{pmatrix} \neq 0, \qquad K\begin{pmatrix} r & r-1 \\ r & \end{pmatrix} = 0, \tag{3.6}$$

so that near this point the left boundary condition effectively becomes that of Fig. 1.

4. The character $\chi_{1,1}$

We first study the spectrum of the transfer matrix $\boldsymbol{T}(u)$ for a lattice of width N and boundary heights $(r, s) = (1, 1)$, as defined by Eq. (2.4). The adjacency condition implies that N must be even. We begin by classifying the zeros of the eigenvalues of $\boldsymbol{T}(u)$, and identifying the characteristics of those eigenvalues in the leading band as $N \to \infty$. This allows us to compute the order-N, order-1 and order-$1/N$ behaviour of all eigenvalues in that band, and we will see that the conformal partition function is given by $Z(q) = \chi_{1,1}(q)$.

4.1. Classification of zeros

From numerical diagonalization of $\boldsymbol{T}(u)$ we are able to classify all eigenvalues according to their zeros in the complex plane. For each eigenvalue we find that – apart from a pair of zeros at $u = \lambda + \xi$ and $u = 5\lambda - \xi$ induced by the left boundary weight – the zeros of the eigenvalues occur on certain fixed lines. Specifically, two types of 1-strings and two types of 2-strings occur. A 1-string is given by a single zero u_j such that

$$\mathrm{Re}(u_j) = \begin{cases} \frac{1}{2}\lambda, & \text{type 1,} \\ 3\lambda, & \text{type 2.} \end{cases} \tag{4.1}$$

A 2-string is a pair of zeros (u_j, u_j') with equal imaginary part and

$$(\mathrm{Re}(u_j), \mathrm{Re}(u_j')) = \begin{cases} (-\frac{1}{2}\lambda, \frac{3}{2}\lambda), & \text{type 1,} \\ (2\lambda, 4\lambda), & \text{type 2.} \end{cases} \tag{4.2}$$

Distributions of zeros for two typical eigenvalues of $\boldsymbol{T}(u)$ for $N = 16$ are depicted in Figs. 2 and 3. We note that for finite N the 2-strings do not fall precisely on the lines given in Eq. (4.2), but that this deviation vanishes as N increases.

Due to the crossing symmetry $\boldsymbol{T}(u) = \boldsymbol{T}(\lambda - u)$, each string occurs with its complex conjugate. We further observe from our numerics that only the exceptional zeros at $u = \lambda + \xi$ and $u = 5\lambda - \xi$ occur on the real axis. Hence, given an eigenvalue, we can denote the number of strings as follows:

$$\begin{aligned} 2m_1 &= \text{number of 1-strings of type 1,} & 2n_1 &= \text{number of 2-strings of type 1,} \\ 2m_2 &= \text{number of 1-strings of type 2,} & 2n_2 &= \text{number of 2-strings of type 2.} \end{aligned} \tag{4.3}$$

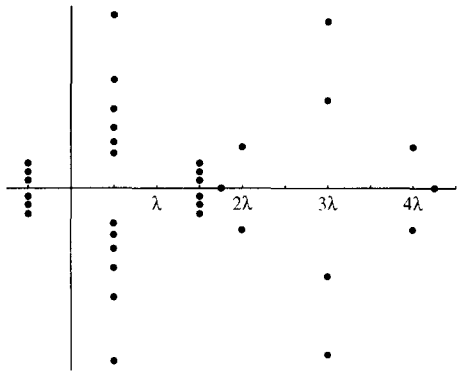

Fig. 2. Zeros of a typical eigenvalue of $\boldsymbol{T}(u)$ in the complex u-plane.

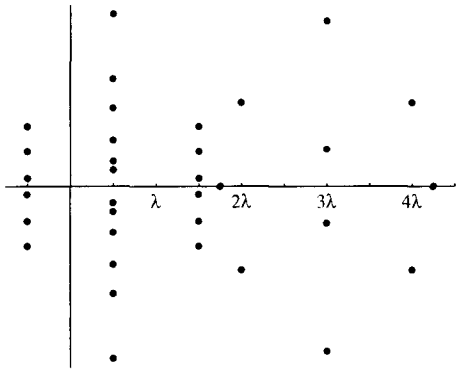

Fig. 3. Zeros of another typical eigenvalue of $\boldsymbol{T}(u)$ in the complex u-plane.

Since each eigenvalue of $\boldsymbol{T}(u)$ has $2N+2$ zeros, we have the completeness relation

$$m_1 + m_2 + 2n_1 + 2n_2 = N. \tag{4.4}$$

In addition, we observe the relation

$$m_2 + n_2 = \tfrac{1}{2}m_1, \tag{4.5}$$

so that both m_1 and m_2 are even (recalling that N is even). These two equations may be recast in the more familiar form of an $(\boldsymbol{m},\boldsymbol{n})$-system [32]

$$\boldsymbol{m} + \boldsymbol{n} = \tfrac{1}{2}(N\boldsymbol{e}_1 + \mathcal{I}\boldsymbol{m}), \tag{4.6}$$

where $\boldsymbol{m} = (m_1, m_2)$, $\boldsymbol{n} = (n_1, n_2)$, $\boldsymbol{e}_1 = (1,0)$, and $\mathcal{I}$ is the A_2 incidence matrix with entries $\mathcal{I}_{j,k} = \delta_{|j-k|,1}$.

For each system size, we find that there are many eigenvalues with the same string content $(\boldsymbol{m},\boldsymbol{n})$. These eigenvalues are distinguished by the relative orderings of the strings of type 1, and the relative orderings of the strings of type 2. Denoting the imaginary parts of the 1-strings of type j by $0 < v_1^{(j)} < \ldots < v_{m_j}^{(j)}$, and the imaginary parts of the 2-strings of type j by $0 < w_1^{(j)} < \ldots < w_{n_j}^{(j)}$, we see that in Fig. 2

$$0 < w_1^{(1)} < w_2^{(1)} < w_3^{(1)} < v_1^{(1)} < v_2^{(1)} < \ldots < v_6^{(1)},$$
$$0 < w_1^{(2)} < v_1^{(2)} < v_2^{(2)}, \tag{4.7}$$

whereas in Fig. 3, which has the same string content,

$$0 < w_1^{(1)} < v_1^{(1)} < v_2^{(1)} < w_2^{(1)} < v_3^{(1)} < w_3^{(1)} < v_4^{(1)} < v_5^{(1)} < v_6^{(1)},$$
$$0 < v_1^{(2)} < w_1^{(2)} < v_2^{(2)}. \tag{4.8}$$

Clearly, the total number of possible orderings for a given $(\boldsymbol{m}, \boldsymbol{n})$ is $\binom{m_1+n_1}{m_1}\binom{m_2+n_2}{m_2}$. Summing over all allowed string contents $(\boldsymbol{m}, \boldsymbol{n})$ using (4.6) then gives

$$\sum_{\substack{m_1 \text{ even} \\ m_2 \text{ even}}} \binom{m_1+n_1}{m_1}\binom{m_2+n_2}{m_2} = A_{1,1}^N, \tag{4.9}$$

which as we see from Eq. (2.5) is indeed the correct number of eigenvalues.

4.2. Characterization of leading eigenvalues

Having classified all eigenvalues of $\boldsymbol{T}$, we would like to calculate the order-$1/N$ corrections to the leading band. The eigenvalues in this band are obtained as follows. For an arbitrary system size $N = N_0$, consider a pattern of zeros labelled by m_1, m_2, n_1 and n_2. Now increase N, keeping m_1, m_2 and n_2 fixed. From the completeness relation (4.4) we see that the number of 2-strings of type 1 must grow linearly with N. In addition, we keep fixed the relative ordering between $\{v_k^{(1)}\}_{k=1}^{m_1}$ and $\{w_k^{(1)}\}_{k=1}^{n_1}$ and the relative ordering between $\{v_k^{(2)}\}_{k=1}^{m_2}$ and $\{w_k^{(2)}\}_{k=1}^{n_2}$. We also specify that the 2-strings of type 1 added as N is increased all have imaginary parts less than $\min\{v_1^{(1)}, w_1^{(1)}, v_1^{(2)}, w_1^{(2)}\}$. To obtain the leading band of eigenvalues in the thermodynamic limit we must finally take $N_0 \to \infty$.

The process of adding 2-strings of type 1 has the effect of pushing the original zeros away from the real u-axis. We observe from our numerics that this growth is logarithmic, and that the limits

$$y_k^{(j)} = \lim_{N\to\infty} (5v_k^{(j)} - \ln N), \qquad z_k^{(j)} = \lim_{N\to\infty} (5w_k^{(j)} - \ln N), \tag{4.10}$$

are well defined.

4.3. Free energies

Before calculating the order-$1/N$ corrections to the leading band of eigenvalues, we need to determine the order-N and order-1 contributions. Because all of the zeros except those on the lines $\mathrm{Re}(u) = -\frac{1}{2}\lambda$ and $\mathrm{Re}(u) = \frac{3}{2}\lambda$ are pushed to infinity logarithmically with N, these contributions are the same for all eigenvalues in the leading band.

Since the number of zeros on the lines $\mathrm{Re}(u) = -\frac{1}{2}\lambda$ and $\mathrm{Re}(u) = \frac{3}{2}\lambda$ grows linearly with N while their extent grows logarithmically, these zeros become dense. Hence in the

thermodynamic limit we consider two distinct regions of analyticity, $-\frac{1}{2}\lambda < \mathrm{Re}(u) < \frac{3}{2}\lambda$ and $\frac{3}{2}\lambda < \mathrm{Re}(u) < \frac{9}{2}\lambda$.

Up to this point our discussion has pertained to the transfer matrix $\boldsymbol{T}$. We now want to use the functional equation (2.7) for the normalized transfer matrix $\boldsymbol{t}$, so we have to consider additional zeros and poles introduced by the normalization factors in Eq. (2.6). The ratio of functions $\gamma_k(u)$ induces poles of order $2N$ at $u = 2\lambda$ and $u = 4\lambda$ and a zero of order $2N$ at $u = 3\lambda$. Likewise, the function $\beta(u)$ induces poles of order 1 at $u = -\frac{1}{2}\lambda$, $u = \frac{3}{2}\lambda$, $u = 2\lambda$ and $u = 4\lambda$, and zeros of order 2 at $u = \frac{1}{2}\lambda$ and $u = 3\lambda$. Finally, the product $\alpha_1(u-\xi)\,\alpha_{-1}(u+\xi)$ implies poles of order 1 at $u = \lambda + \xi$ and $u = 5\lambda - \xi$. Note that these last poles of order 1 cancel the anomalous zeros on the real axis induced by the boundary weight.

Writing an eigenvalue of $\boldsymbol{t}$ as t, we isolate the order-N and order-1 behaviour,

$$t(u) = f(u)\, g(u)\, l(u), \tag{4.11}$$

where the functions f and g are defined by

$$[f(u)]^{1/N} = \lim_{N\to\infty} [t(u)]^{1/N}, \qquad g(u) = \lim_{N\to\infty} t(u)/f(u). \tag{4.12}$$

The order-N behaviour of the functional equation (2.7) is then [9,33]

$$f(u)\, f(u+\lambda) = 1, \tag{4.13}$$

for $-\frac{1}{2}\lambda < u < \frac{1}{2}\lambda$ or $\frac{3}{2}\lambda < u < \frac{7}{2}\lambda$. The solution of this equation in accordance with the order-N analyticity is

$$f(u) = \begin{cases} 1, & -\frac{1}{2}\lambda < u < \frac{3}{2}\lambda, \\ \cot^{2N}(\frac{5}{2}u), & \frac{3}{2}\lambda < u < \frac{9}{2}\lambda. \end{cases} \tag{4.14}$$

This solution in turn implies the order-1 functional equation

$$g(u)\, g(u+\lambda) = \begin{cases} 1, & -\frac{1}{2}\lambda < u < \frac{1}{2}\lambda, \\ 1 + g(u-2\lambda), & \frac{3}{2}\lambda < u < \frac{7}{2}\lambda. \end{cases} \tag{4.15}$$

In the interval $-\frac{1}{2}\lambda < u < \frac{3}{2}\lambda$, the solution in accordance with the order-1 analyticity is given by

$$g(u) = -\tan^2(\tfrac{5}{2}u - \tfrac{\pi}{4}). \tag{4.16}$$

The solution inside $\frac{3}{2}\lambda < u < \frac{9}{2}\lambda$ can be obtained similarly, but will not concern us as it does not enter the calculation of the order-$1/N$ corrections.

4.4. *Computation of the order-1/N corrections*

For convenience, we start by selecting a line of constant real part within each of the two strips in the u-plane. For the functions t, f, g and l, it is then natural to define

$$h_1(x) = h(\tfrac{1}{2}\lambda + \tfrac{1}{5}\mathrm{i}x), \qquad \text{for } |\mathrm{Im}(x)| < \pi,$$

$$h_2(x) = h(3\lambda + \tfrac{1}{5}\mathrm{i}x), \qquad \text{for } |\operatorname{Im}(x)| < \tfrac{3}{2}\pi, \tag{4.17}$$

as well as

$$H_1(x) = 1 + h_1(x), \qquad H_2(x) = 1 + h_2(x). \tag{4.18}$$

Substituting (4.11) into the functional equation (2.7), and using Eqs. (4.13) and (4.15), we obtain

$$\begin{aligned} &l_1(x - \tfrac{1}{2}\mathrm{i}\pi) l_1(x + \tfrac{1}{2}\mathrm{i}\pi) = T_2(x), \\ &l_2(x - \tfrac{1}{2}\mathrm{i}\pi) l_2(x + \tfrac{1}{2}\mathrm{i}\pi) = T_1(x)/G_1(x). \end{aligned} \tag{4.19}$$

For a given eigenvalue of string content $(\boldsymbol{m}, \boldsymbol{n})$, the function $l_j(x)$ has m_j pairs of zeros inside the strip $|\operatorname{Im}(x)| < \pi$. Hence

$$l_j(x) \prod_{k=1}^{m_j} \coth[\tfrac{1}{2}(5v_k^{(j)} - x)] \coth[\tfrac{1}{2}(5v_k^{(j)} + x)], \qquad \text{for } j = 1, 2, \tag{4.20}$$

is free of poles and zeros inside this strip. Taking the Fourier transform of the logarithmic derivative of Eq. (4.19) thus gives, for $|\operatorname{Im}(x)| < \pi$,

$$\ln l_1(x) = \sum_{k=1}^{m_1} \ln\bigl(\tanh[\tfrac{1}{2}(5v_k^{(1)} - x)] \tanh[\tfrac{1}{2}(5v_k^{(1)} + x)]\bigr) + k * \ln T_2(x) + D_1, \tag{4.21}$$

$$\begin{aligned} \ln l_2(x) = &\sum_{k=1}^{m_2} \ln\bigl(\tanh[\tfrac{1}{2}(5v_k^{(2)} - x)] \tanh[\tfrac{1}{2}(5v_k^{(2)} + x)]\bigr) + k * \ln(T_1/G_1)(x) \\ &+ D_2, \end{aligned} \tag{4.22}$$

where $f * g$ denotes a convolution and the kernel k is

$$k(x) = \frac{1}{2\pi \cosh x}. \tag{4.23}$$

Before we can determine the integration constants D_1 and D_2, we have to fix the branches of the logarithms of l_1 and l_2. We first observe from numerical diagonalization of $\boldsymbol{T}(u)$ that the complex function $l_j(x - \mathrm{i}\varepsilon)$, where $\varepsilon > 0$, winds $\frac{1}{2}m_j$ times around the origin anticlockwise as x increases from zero to infinity. An example of this winding is given in Figs. 4 and 5. In selecting branches of $\ln l_j$, we regard $l_j(x)$ as $\lim_{\varepsilon \to 0} l_j(x - \mathrm{i}\varepsilon)$. At each point $x = \pm 5v_k^{(j)}$ the real function $l_j(x)$ changes sign. We specify that between $x = \pm 5v_1^{(j)}$ the logarithm corresponds to the principal branch, so that for $k = 1, \ldots, m_j - 1$

$$\operatorname{Im}\bigl(\ln l_j(x)\bigr) = \lim_{\varepsilon \to 0} \operatorname{Im}\bigl(\ln l_j(x - \mathrm{i}\varepsilon)\bigr) = \begin{cases} 0, & 0 \leqslant x < 5v_1^{(j)}, \\ k\pi, & 5v_k^{(j)} < x < 5v_{k+1}^{(j)}, \\ m_j\pi, & 5v_{m_j}^{(j)} < x. \end{cases} \tag{4.24}$$

We note that this definition also implies that $\operatorname{Im}(\ln l_j(5v_k^{(j)})) = (k - \frac{1}{2})\pi$.

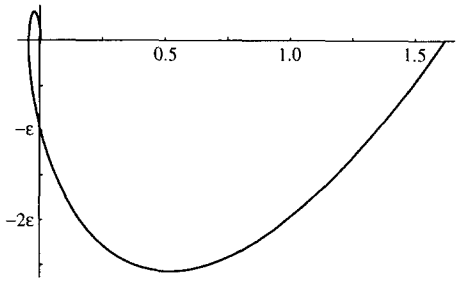

Fig. 4. The function $I_1(x - i\varepsilon)$ in the complex plane between $x = 0$ and $x = \infty$, corresponding to the eigenvalue depicted in Fig. 2. As x increases, the function winds anticlockwise.

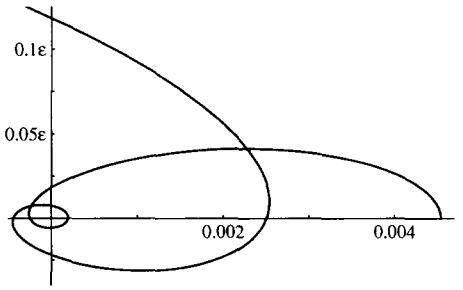

Fig. 5. Magnification of Fig. 4 in the vicinity of the origin. The total of six intersections with the imaginary axis corresponds to $m_1 = 6$ in Fig. 2.

We are now able to determine D_1 and D_2, but it is convenient first to take the scaling limit. Guided by the function f_2, which behaves as

$$\lim_{N\to\infty} f_2(x + \ln N) = \exp(-4e^{-x}), \tag{4.25}$$

we assume the general scaling forms

$$\hat{h}(x) = \lim_{N\to\infty} h(x + \ln N). \tag{4.26}$$

It will be important later to note that

$$\lim_{x\to\infty} \hat{h}(x) = \lim_{x\to\infty} h(x), \qquad \lim_{x\to-\infty} \hat{h}(x) = \lim_{x\to-\infty} \lim_{N\to\infty} h(x), \tag{4.27}$$

as may be explicitly verified for the function f_2.

Now taking the scaling limit of (4.21) and (4.22) gives

$$\ln \hat{t}_1(x) = \sum_{k=1}^{m_1} \ln\bigl(\tanh[\tfrac{1}{2}(y_k^{(1)} - x)]\bigr) + k * \ln \hat{T}_2(x), \tag{4.28}$$

$$\ln \hat{t}_2(x) = -4e^{-x} + \sum_{k=1}^{m_2} \ln\bigl(\tanh[\tfrac{1}{2}(y_k^{(2)} - x)]\bigr) + k * \ln \hat{T}_1(x). \tag{4.29}$$

To obtain these expressions we have used the factorization (4.11), Eqs. (4.10) and (4.25), the property

$$(k * \ln H)(\infty) = \ln H(\infty) \int_{-\infty}^{\infty} k(y)\, dy = \tfrac{1}{2} \ln H(\infty) \tag{4.30}$$

and the limits $x \to \infty$ of Eqs. (2.7), (4.13) and (4.15). From these and Eq. (4.24) we have $D_1 = D_2 = 0$.

We now return to the calculation of the finite-size corrections and express the order-$1/N$ contributions to $\ln l_1$ in terms of scaling functions. Taking the first term on the right-hand side of Eq. (4.21), we use Eq. (4.10) to write

$$\sum_{k=1}^{m_1} \ln\bigl(\tanh[\tfrac{1}{2}(5v_k^{(1)} - x)]\tanh[\tfrac{1}{2}(5v_k^{(1)} + x)]\bigr) = -\frac{4}{N}\cosh x \sum_{k=1}^{m_1} \mathrm{e}^{-y_k^{(1)}} + \mathrm{o}\Bigl(\frac{1}{N}\Bigr). \tag{4.31}$$

Next we consider

$$\begin{aligned} k * \ln T_2(x) &= \int_0^{\infty} [k(x-y) + k(x+y)] \ln T_2(y)\, dy \\ &= \int_{-\ln N}^{\infty} [k(x-y-\ln N) + k(x+y+\ln N)] \ln T_2(y+\ln N)\, dy \end{aligned} \tag{4.32}$$

and assume that this can be replaced by

$$k * \ln T_2(x) = \frac{2}{\pi N}\cosh x \int_{-\infty}^{\infty} \mathrm{e}^{-y} \ln \hat{T}_2(y)\, dy + \mathrm{o}\Bigl(\frac{1}{N}\Bigr). \tag{4.33}$$

This assumption can be verified explicitly when T_2 is replaced by $1 + f_2$. Hence, combining Eqs. (4.21), (4.31) and (4.33), we have to leading order

$$\ln l_1(x) = -\frac{4}{N}\cosh x \Bigl[\sum_{k=1}^{m_1} \mathrm{e}^{-y_k^{(1)}} - \frac{1}{2\pi}\int_{-\infty}^{\infty} \mathrm{e}^{-y} \ln \hat{T}_2(y)\, dy\Bigr]. \tag{4.34}$$

We now rewrite this expression by manipulating the functional equations (4.28) and (4.29). Evaluating (4.28) at $x = y_k^{(2)} - \frac{1}{2}\mathrm{i}\pi$ and (4.29) at $x = y_k^{(1)} - \frac{1}{2}\mathrm{i}\pi$ gives

$$\begin{aligned} 0 = \frac{1}{2\pi}\int_{-\infty}^{\infty} \frac{\ln \hat{T}_2(y)}{\sinh(y_k^{(2)} - y)}\, dy - \mathrm{i}\sum_{l=1}^{m_1} \ln\bigl(\tanh[\tfrac{1}{2}(y_l^{(1)} - y_k^{(2)} + \tfrac{1}{2}\mathrm{i}\pi)]\bigr) \\ + \mathrm{i}\ln \hat{t}_1(y_k^{(2)} - \tfrac{1}{2}\mathrm{i}\pi) \end{aligned} \tag{4.35}$$

and

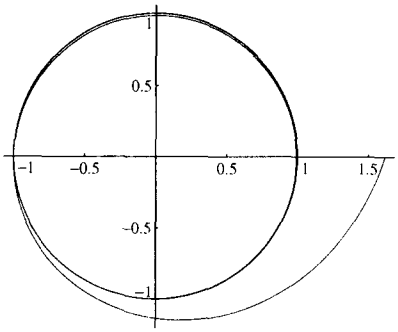

Fig. 6. The function $t_2(x - \frac{1}{2}i\pi)$ in the complex plane between $x = 0$ and $x = \infty$, corresponding to the eigenvalue depicted in Fig. 2. As x decreases from infinity to $w_1^{(1)} > 0$, the argument of the function decreases by a total of $(2m_1 + 2n_1 - 1)\pi = 17\pi$. The function $t_1(x - \frac{1}{2}i\pi)$ behaves similarly, but with a total decrease in argument of $(2m_2 + 2n_2 - 1)\pi = 5\pi$.

$$4e^{-y_k^{(1)}} = \frac{1}{2\pi}\int_{-\infty}^{\infty} \frac{\ln \hat{T}_1(y)}{\sinh(y_k^{(1)} - y)}\,dy - i\sum_{l=1}^{m_2} \ln\bigl(\tanh[\tfrac{1}{2}(y_l^{(2)} - y_k^{(1)} + \tfrac{1}{2}i\pi)]\bigr) + i\ln \hat{t}_2(y_k^{(1)} - \tfrac{1}{2}i\pi). \tag{4.36}$$

The scaling limit of the functional equation (2.7) implies that

$$\hat{t}_1(y_k^{(2)} - \tfrac{1}{2}i\pi) = \hat{t}_1(z_k^{(2)} - \tfrac{1}{2}i\pi) = -1,$$
$$\hat{t}_2(y_k^{(1)} - \tfrac{1}{2}i\pi) = \hat{t}_2(z_k^{(1)} - \tfrac{1}{2}i\pi) = -1. \tag{4.37}$$

We now determine the branch of the logarithm at the points $\hat{t}_j(y_k^{(j')} - \frac{1}{2}i\pi)$, where $j' = 3 - j$. Decreasing x from infinity in the function $\hat{t}_j(x - \frac{1}{2}i\pi)$, we encounter the $m_{j'} + n_{j'}$ points at which $\hat{t}_j = -1$. Between successive encounters $\hat{t}_j$ decreases its argument by 2π, a property which can be observed numerically for t_j as in Fig. 6. Since Eq. (4.24) implies $\mathrm{Im}\bigl(\ln \hat{t}_j(\infty)\bigr) = m_j\pi$, we see that

$$\ln \hat{t}_1(y_k^{(2)} - \tfrac{1}{2}i\pi) = (2k + m_1 - 2m_2 - 1 - 2I_k^{(2)})i\pi,$$
$$\ln \hat{t}_2(y_k^{(1)} - \tfrac{1}{2}i\pi) = (2k + m_2 - 2m_1 - 1 - 2I_k^{(1)})i\pi, \tag{4.38}$$

where $I_k^{(j)}$ is the number of $z_l^{(j)}$ greater than $y_k^{(j)}$. Since $y_{k+1}^{(j)} > y_k^{(j)}$, the integers $I_k^{(j)}$ must satisfy

$$n_j \geqslant I_1^{(j)} \geqslant I_2^{(j)} \geqslant \ldots \geqslant I_{m_j}^{(j)} \geqslant 0. \tag{4.39}$$

If we now sum Eq. (4.35) from $k = 1$ to m_2, Eq. (4.36) from $k = 1$ to m_1 and use the relation

$$\ln\bigl(\tanh(\tfrac{1}{4}i\pi + x)\bigr) + \ln\bigl(\tanh(\tfrac{1}{4}i\pi - x)\bigr) = i\pi, \tag{4.40}$$

we arrive at

$$\frac{4}{\pi}\sum_{k=1}^{m_1} e^{-y_k^{(1)}} = \tfrac{1}{2}\boldsymbol{m}C\boldsymbol{m} + \sum_{j=1}^{2}\sum_{k=1}^{m_j}\left[2I_k^{(j)} + \frac{1}{2\pi^2}\int_{-\infty}^{\infty}\frac{\ln\hat{T}_j(y)}{\sinh(y_k^{(j)}-y)}\,dy\right], \tag{4.41}$$

where C is the A_2 Cartan matrix with entries given by $C_{j,k} = 2\delta_{j,k} - \delta_{|j-k|,1}$. Substituting (4.41) into Eq. (4.34) gives

$$\ln l_1(x) = -\frac{\pi}{N}\cosh x\left(\tfrac{1}{2}\boldsymbol{m}C\boldsymbol{m} + \sum_{j=1}^{2}\sum_{k=1}^{m_j}\left[2I_k^{(j)} + \frac{1}{2\pi^2}\int_{-\infty}^{\infty}\frac{\ln\hat{T}_j(y)}{\sinh(y_k^{(j)}-y)}\,dy\right] - \frac{2}{\pi^2}\int_{-\infty}^{\infty} e^{-y}\ln\hat{T}_2(y)\,dy\right). \tag{4.42}$$

It remains to evaluate the integrals in Eq. (4.42). Following Ref. [9], we consider the quantities

$$S_j = \int_{-\infty}^{\infty}\left([\ln\hat{t}_j(x)]'\ln\hat{T}_j(x) - \ln\hat{t}_j(x)\,[\ln\hat{T}_j(x)]'\right)dx, \qquad \text{for } j = 1,2. \tag{4.43}$$

On the one hand we can use the explicit expressions for $\ln\hat{t}_j$ given in Eqs. (4.28) and (4.29) to write

$$S_1 + S_2 = 8\int_{-\infty}^{\infty} e^{-x}\ln\hat{T}_2(x)\,dx - \sum_{j=1}^{2}\left[i\pi m_j\ln\hat{T}_j(\infty) + 2\sum_{k=1}^{m_j}\int_{-\infty}^{\infty}\frac{\ln\hat{T}_j(x)}{\sinh(y_k^{(j)}-x)}\,dx\right], \tag{4.44}$$

where due to the symmetry $k(x) = k(-x)$ all terms involving the kernel have cancelled.

On the other hand, we can change integration variables in Eq. (4.43) to evaluate S_j directly. Dividing the line of integration into the $m_j + 1$ intervals between $-\infty < y_1^{(j)} < \ldots < y_{m_j}^{(j)} < \infty$, we note that for all $k = 1, \ldots, m_j - 1$,

$$\int_{y_k^{(j)}}^{y_{k+1}^{(j)}}\left([\ln\hat{t}_j(x)]'\ln\hat{T}_j(x) - \ln\hat{t}_j(x)\,[\ln\hat{T}_j(x)]'\right)dx = \int_{\hat{t}_j(y_k^{(j)})}^{\hat{t}_j(y_{k+1}^{(j)})}\left(\frac{\ln(1+x)}{x} - \frac{\ln x + i\pi k}{1+x}\right)dx = 0. \tag{4.45}$$

Hence we are left with

$$S_j = \int_{\hat{t}_j(-\infty)}^{0} \left(\frac{\ln(1+x)}{x} - \frac{\ln x}{1+x} \right) dx + \int_{0}^{\hat{t}_j(\infty)} \left(\frac{\ln(1+x)}{x} - \frac{\ln x + i\pi m_j}{1+x} \right) dx$$

$$= \int_{\hat{t}_j(-\infty)}^{\hat{t}_j(\infty)} \left(\frac{\ln(1+x)}{x} - \frac{\ln x}{1+x} \right) dx - i\pi m_j \ln \hat{T}_j(\infty). \tag{4.46}$$

From Eqs. (2.11), (4.14), (4.16) and (4.27), we obtain the limits

$$\hat{t}_1(\infty) = \hat{t}_2(\infty) = 2\cos\lambda, \qquad \hat{t}_1(-\infty) = g_1(-\infty) = 1,$$
$$\hat{t}_2(-\infty) = f_2(-\infty) = 0, \tag{4.47}$$

which give, using the values of the Rogers dilogarithm in the appendix,

$$S_1 + S_2 + i\pi \sum_{j=1}^{2} m_j \ln \hat{T}_j(\infty) = 4L\left(\frac{1}{2\cos\lambda} \right) - 2L(\tfrac{1}{2}) = \tfrac{7}{30}\pi^2. \tag{4.48}$$

Equating (4.44) and (4.48), we finally arrive at

$$\frac{2}{\pi^2} \int_{-\infty}^{\infty} e^{-x} \ln \hat{T}_2(x)\, dx + \frac{1}{2\pi^2} \sum_{j=1}^{2} \sum_{k=1}^{m_j} \frac{\ln \hat{T}_j(x)}{\sinh(y_k^{(j)} - x)}\, dx = \tfrac{7}{120}. \tag{4.49}$$

Substituting Eq. (4.49) into Eq. (4.42), then recalling Eq. (4.17), we have

$$\ln l(u) = \frac{2\pi}{N} \sin(5u) \left[\tfrac{7}{240} - \tfrac{1}{4}\boldsymbol{m}C\boldsymbol{m} - \sum_{j=1}^{2} \sum_{k=1}^{m_j} I_k^{(j)} \right]. \tag{4.50}$$

Since m_1 and m_2 are even, the "minimal" solution of Eq. (4.6) is $m_1 = m_2 = 0$. Thus comparison of (4.50) with Eq. (3.3) shows that $c = \frac{7}{10}$ and $\Delta = 0$, and hence that the integer n is to be identified with

$$n = \tfrac{1}{4}\boldsymbol{m}C\boldsymbol{m} + \sum_{j=1}^{2} \sum_{k=1}^{m_j} I_k^{(j)}. \tag{4.51}$$

From Eq. (3.4) we see that to calculate the conformal partition function $Z(q)$ we must sum over q^n. From Eq. (4.51), this amounts to summing over all allowed values $\boldsymbol{m}$ and $I_k^{(j)}$. We first perform the sum over $I_k^{(j)}$ using the restrictions (4.39)

$$\sum_{I_1^{(j)}=0}^{n_j} \sum_{I_2^{(j)}=0}^{I_1^{(j)}} \cdots \sum_{I_{m_j}^{(j)}=0}^{I_{m_j-1}^{(j)}} q^{I_1^{(j)} + \ldots + I_{m_j}^{(j)}} = \begin{bmatrix} m_j + n_j \\ m_j \end{bmatrix}. \tag{4.52}$$

Here the q-binomial coefficient is defined by

$$\begin{bmatrix} m+n \\ m \end{bmatrix} = \begin{cases} (q)_{m+n}/(q)_m(q)_n, & m, n \geqslant 0, \\ 0, & \text{otherwise}, \end{cases} \tag{4.53}$$

with $(q)_m = (1-q)\cdots(1-q^m)$ for $m \geqslant 1$ and $(q)_0 = 1$. Now summing over $\boldsymbol{m}$ gives

$$Z_{N_0}(q) = q^{-\frac{c}{24}} \sum_{\substack{m_1 \text{ even} \\ m_2 \text{ even}}} q^{\frac{1}{4}\boldsymbol{m}C\boldsymbol{m}} \begin{bmatrix} m_1+n_1 \\ m_1 \end{bmatrix} \begin{bmatrix} m_2+n_2 \\ m_2 \end{bmatrix}, \tag{4.54}$$

with $\boldsymbol{m}+\boldsymbol{n} = \frac{1}{2}(N_0\boldsymbol{e}_1 + \mathcal{I}\boldsymbol{m})$. Following our description of the leading band of eigenvalues in Section 4.2, we take $N_0 \to \infty$ to obtain

$$Z(q) = q^{-\frac{c}{24}} \sum_{\substack{m_1 \text{ even} \\ m_2 \text{ even}}} \frac{q^{\frac{1}{4}\boldsymbol{m}C\boldsymbol{m}}}{(q)_{m_1}} \begin{bmatrix} \frac{1}{2}m_1 \\ m_2 \end{bmatrix} = \chi_{1,1}(q). \tag{4.55}$$

Thus we see that the conformal partition function for the $(r,s) = (1,1)$ boundary condition is the $\chi_{1,1}(q)$ Virasoro character, and that it arises naturally in its fermionic representation [34].

5. The character $\chi_{1,2}$

We next consider a lattice with boundary heights $(r,s) = (1,2)$. We will see that the main difference in comparison to the $(1,1)$ boundary occurs in the classification of the transfer matrix eigenvalues, and we find the conformal partition function $Z(q) = \chi_{1,2}(q)$.

5.1. Classification of zeros

Our numerics show that the zero patterns of eigenvalues of $\boldsymbol{T}$ with the $(1,2)$ boundary condition are qualitatively the same as those with the $(1,1)$ boundary condition. That is, the same four string types occur, and the same zeros on the real u-axis are induced by the left boundary weight. Therefore we again define $(\boldsymbol{m},\boldsymbol{n})$ by Eq. (4.3). The difference between the two boundary conditions lies in the orderings of the strings of type 1. Previously, given a string content $(\boldsymbol{m},\boldsymbol{n})$, eigenvalues corresponding to all $\binom{m_1+n_1}{m_1}$ orderings of strings of type 1 were seen to occur. In this case, however, we observe that for certain string contents, the 1-string of type 1 furthest from the real u-axis is "frozen", so that no eigenvalue occurs with $v_{m_1}^{(1)} < w_{n_1}^{(1)}$. Hence for these contents, only $\binom{m_1+n_1-1}{m_1-1}$ orderings of the strings of type 1 are permitted.

To treat both cases simultaneously, we introduce a variable $\sigma = \pm 1$, with $\sigma = 1$ for contents with a frozen 1-string, and $\sigma = -1$ for the other contents. We then find that the strings satisfy the $(\boldsymbol{m},\boldsymbol{n})$-system

$$m_1 + n_1 = \tfrac{1}{2}(N + m_2 + \sigma), \qquad m_2 + n_2 = \tfrac{1}{2}(m_1 - \sigma). \tag{5.1}$$

Since N is odd, this implies that m_1 is odd and m_2 is even. Using (5.1), the total number of eigenvalues is correctly computed to be

$$\sum_{\sigma} \sum_{\substack{m_1 \text{ odd} \\ m_2 \text{ even}}} \binom{m_1 + n_1 - \delta_{\sigma,1}}{m_1 - \delta_{\sigma,1}} \binom{m_2 + n_2}{m_2} = A^N_{1,2}. \tag{5.2}$$

5.2. *Computation of the order-1/N corrections*

As the order-N analyticity is independent of the choice of boundary conditions, the solution of the functional equation (4.13) for f is once again given by (4.14). The order-1 analyticity, and hence the solution of Eq. (4.15) for g, does depend on the boundary conditions, but in this case it is unchanged from the description of Section 4.3. Thus the function g for the $(1,2)$ boundary is again given by Eq. (4.16).

Recalling the definition of l_j from Eqs. (4.11) and (4.17), and proceeding with the Fourier transformation as performed in Section 4.4, we again obtain Eqs. (4.21) and (4.22). Examination of the winding of the function $l_j(x - \mathrm{i}\varepsilon)$ shows the same behaviour as before, and we choose branches of the logarithms in accordance with Eq. (4.24). Now taking the scaling limit of (4.21) and (4.22), and again using the limits $x \to \infty$ of Eqs. (2.7), (4.13) and (4.15) in conjunction with (4.10) and (4.24), we obtain

$$\begin{aligned} \ln \hat{t}_1(x) &= \sum_{k=1}^{m_1} \ln\bigl(\tanh[\tfrac{1}{2}(y_k^{(1)} - x)]\bigr) + k * \ln \hat{T}_2(x), \\ \ln[-\hat{t}_2(x)] &= -4\mathrm{e}^{-x} + \sum_{k=1}^{m_2} \ln\bigl(\tanh[\tfrac{1}{2}(y_k^{(2)} - x)]\bigr) + k * \ln \hat{T}_1(x). \end{aligned} \tag{5.3}$$

We note that since the limit $\lim_{iu \to \infty} t(u)_{a,a}$ in Eq. (2.11) is negative when $s = 2$, our signs inside the logarithms of $\hat{t}_1$ and $\hat{t}_2$ are such that

$$\mathrm{Im}\bigl(\ln \hat{t}_1(\infty)\bigr) = m_1\pi, \qquad \mathrm{Im}\bigl(\ln[-\hat{t}_2(\infty)]\bigr) = m_2\pi \tag{5.4}$$

are consistent with the parities of m_1 and m_2.

Following the same procedure as in Section 4.4, we will use (5.3) to rewrite the order-$1/N$ term (4.34). The crucial step, and the one at which differences between this and the $(1,1)$ boundary case are evident, is the determination of $\ln \hat{t}_1(y_k^{(2)} - \frac{1}{2}\mathrm{i}\pi)$ and $\ln[-\hat{t}_2(y_k^{(1)} - \frac{1}{2}\mathrm{i}\pi)]$. When $\sigma = -1$, the behaviours of $t_1(x - \frac{1}{2}\mathrm{i}\pi)$ and $t_2(x - \frac{1}{2}\mathrm{i}\pi)$ are given respectively in Figs. 7 and 8. When $\sigma = 1$, the qualitative features of the two plots are interchanged. In each case the arguments are decreasing as x decreases from infinity, but we see that in Fig. 7 the function first passes through the point -1 with the same argument as at $x = \infty$, while in Fig. 8 the function's argument has decreased by 2π at the corresponding point. Recalling Eq. (5.4), we therefore see that

$$\begin{aligned} \ln \hat{t}_1(y_k^{(2)} - \tfrac{1}{2}\mathrm{i}\pi) &= (2k + m_1 - 2m_2 - \sigma - 1 - 2I_k^{(2)})\mathrm{i}\pi, \\ \ln[-\hat{t}_2(y_k^{(1)} - \tfrac{1}{2}\mathrm{i}\pi)] &= (2k + m_2 - 2m_1 + \sigma - 1 - 2I_k^{(1)})\mathrm{i}\pi, \end{aligned} \tag{5.5}$$

where $I_k^{(j)}$ is the number of the $z_l^{(j)}$ greater than $y_k^{(j)}$. The integers $I_k^{(j)}$ again satisfy the restrictions (4.39), but with the additional restriction $I_{m_1}^{(1)} = 0$ when $\sigma = 1$.

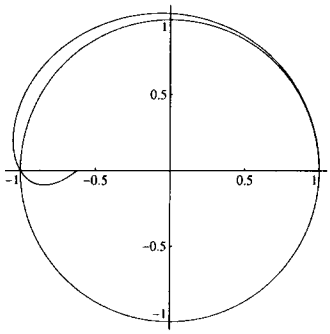

Fig. 7. The function $t_1(x-\frac{1}{2}i\pi)$ in the complex plane between $x=0$ and $x=\infty$. As x decreases the winding is clockwise.

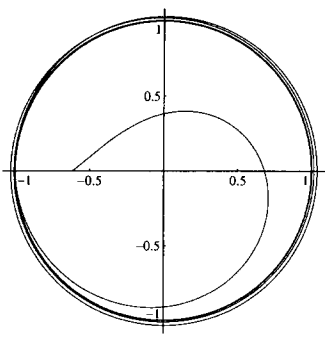

Fig. 8. The function $t_2(x-\frac{1}{2}i\pi)$ in the complex plane between $x=0$ and $x=\infty$. As x decreases the winding is clockwise.

With the branches of the logarithms in (5.5), the manipulation of (4.21) leads to the expression

$$\ln l_1(x) = -\frac{\pi}{N}\cosh x\Bigg(\tfrac{1}{2}\boldsymbol{mCm} - (m_1 - m_2)\sigma + \sum_{j=1}^{2}\sum_{k=1}^{m_j}\Bigg[2I_k^{(j)} + \frac{1}{2\pi^2}\int_{-\infty}^{\infty}\frac{\ln\hat{T}_j(y)}{\sinh(y_k^{(j)}-y)}\,dy\Bigg] - \frac{2}{\pi^2}\int_{-\infty}^{\infty}\mathrm{e}^{-y}\ln\hat{T}_2(y)\,dy\Bigg). \tag{5.6}$$

This corresponds to Eq. (4.42) of Section 4.4. As in that section, we evaluate the integrals in Eq. (5.6) by considering

$$\sum_{j=1}^{2}\int_{-\infty}^{\infty}\Big([\ln\hat{t}_j(x)]'\ln\hat{T}_j(x) - \ln[\pm\hat{t}_j(x)]\,[\ln\hat{T}_j(x)]'\Big)\,dx. \tag{5.7}$$

Substituting the expressions (5.3) for $\ln\hat{t}_1$ and $\ln[-\hat{t}_2]$ leads once again to Eq. (4.44). Equating this to the expression obtained by changing variables of integration and using

the limits

$$\hat{t}_1(\infty) = \hat{t}_2(\infty) = 2\cos(3\lambda), \qquad \hat{t}_1(-\infty) = 1, \qquad \hat{t}_2(-\infty) = 0, \tag{5.8}$$

we arrive at

$$\frac{2}{\pi^2}\int_{-\infty}^{\infty} e^{-x}\ln\hat{T}_2(x)\,dx + \frac{1}{2\pi^2}\sum_{j=1}^{2}\sum_{k=1}^{m_j}\frac{\ln\hat{T}_j(x)}{\sinh(y_k^{(j)}-x)}\,dx$$
$$= -\frac{1}{4\pi^2}\left[4L\big(-2\cos(3\lambda)\big) + 2L\big(\tfrac{1}{2}\big)\right] = -\tfrac{17}{120}. \tag{5.9}$$

Now substituting (5.9) into Eq. (5.6), we obtain

$$\ln I(u) = -\frac{2\pi}{N}\sin(5u)\left[\tfrac{17}{240} + \tfrac{1}{4}\boldsymbol{m}C\boldsymbol{m} - \tfrac{1}{2}(m_1 - m_2)\sigma + \sum_{j=1}^{2}\sum_{k=1}^{m_j} I_k^{(j)}\right]. \tag{5.10}$$

The minimal solution of Eq. (5.1) is $m_1 = 1$ and $m_2 = 0$ with $\sigma = 1$, so in this case $\Delta = \frac{1}{10}$ and the integer n of Eq. (3.3) is given by

$$n = \tfrac{1}{4}\boldsymbol{m}C\boldsymbol{m} - \tfrac{1}{2}(m_1 - m_2)\sigma + \sum_{j=1}^{2}\sum_{k=1}^{m_j} I_k^{(j)}. \tag{5.11}$$

Summing over all eigenvalues in the leading band gives, recalling the restrictions on the integers $I_k^{(j)}$,

$$Z_{N_0}(q) = q^{-\frac{c}{24}+\Delta_{1,2}}\sum_{\sigma}\sum_{\substack{m_1\ \text{odd}\\ m_2\ \text{even}}} q^{\frac{1}{4}\boldsymbol{m}C\boldsymbol{m}-\frac{1}{2}(m_1-m_2)\sigma}\begin{bmatrix} m_1+n_1-\delta_{\sigma,1}\\ m_1-\delta_{\sigma,1}\end{bmatrix}\begin{bmatrix} m_2+n_2\\ m_2\end{bmatrix}. \tag{5.12}$$

Eliminating n_1 and n_2 using Eq. (5.1), we employ the standard q-binomial recurrence

$$\begin{bmatrix} N\\ m\end{bmatrix} = \begin{bmatrix} N-1\\ m-1\end{bmatrix} + q^m\begin{bmatrix} N-1\\ m\end{bmatrix} \tag{5.13}$$

to perform the sum over σ. We thus obtain

$$Z_{N_0}(q) = q^{-\frac{c}{24}+\Delta_{1,2}}\sum_{\substack{m_1\ \text{even}\\ m_2\ \text{even}}} q^{\frac{1}{4}\boldsymbol{m}C\boldsymbol{m}-\frac{1}{2}m_1}\begin{bmatrix}\frac{1}{2}(N_0+m_2+1)\\ m_1\end{bmatrix}\begin{bmatrix}\frac{1}{2}m_1\\ m_2\end{bmatrix}. \tag{5.14}$$

Finally, taking $N_0 \to \infty$ gives

$$Z(q) = q^{-\frac{c}{24}+\Delta_{1,2}}\sum_{\substack{m_1\ \text{even}\\ m_2\ \text{even}}}\frac{q^{\frac{1}{4}\boldsymbol{m}C\boldsymbol{m}-\frac{1}{2}m_1}}{(q)_{m_1}}\begin{bmatrix}\frac{1}{2}m_1\\ m_2\end{bmatrix}, \tag{5.15}$$

which is the $\chi_{1,2}(q)$ Virasoro character [34].

6. The character $\chi_{2,1}$

6.1. Classification of zeros

Under the boundary condition $(2,1)$ the zeros of eigenvalues of $\boldsymbol{T}$ again form the same four string types defined in Section 4.1. In addition to the strings, however, we find that some eigenvalues have zeros on the real u-axis. Such eigenvalues have either a single pair of zeros at $u = 3\lambda \pm \alpha$, or a single quadruplet of zeros at $u = 2\lambda \pm \alpha$ and $u = 4\lambda \pm \alpha$. The numbers α satisfy $0 < \alpha < \frac{1}{2}\lambda$, and are in general different for each eigenvalue. We make the crucial observation that if we fix a set of eigenvalues for an arbitrary system size N_0, and increase the system size by adding 2-strings of type 1 in accordance with the description of the leading band, then for each eigenvalue there exists a K such that $\alpha = 0$ for all $N > K$. Indeed, we see that each pair of real zeros becomes a 1-string of type 2, and that each quadruplet of real zeros becomes a 2-string of type 2.

It is therefore clear that any zeros on the real u-axis should be interpreted as forming strings of type 2. With this interpretation, and with the definitions of Eq. (4.3), we observe that the strings satisfy the $(\boldsymbol{m},\boldsymbol{n})$-system

$$m_1 + n_1 = \tfrac{1}{2}(N + m_2), \qquad m_2 + n_2 = \tfrac{1}{2}(m_1 + 1), \tag{6.1}$$

so that m_1 and m_2 are odd. Using (6.1) we correctly compute

$$\sum_{\substack{m_1 \text{ odd} \\ m_2 \text{ odd}}} \binom{m_1 + n_1}{m_1} \binom{m_2 + n_2}{m_2} = A^N_{2,1}. \tag{6.2}$$

6.2. Free energies

The order-N behaviour is, of course, the same as for the previous two boundary conditions, but the boundary spin $r = 2$ induces different order-1 analyticity on the real u-axis. We see from Section 6.1 that in the limit $N \to \infty$ the eigenvalues of $\boldsymbol{T}$ in the leading band are free of zeros on the real u-axis. However, the product $\alpha_2(u-\xi)\,\alpha_{-2}(u+\xi)$ in the normalization (2.6) of $\boldsymbol{t}$ now introduces zeros of order 1 at $u = \xi - \lambda$ and $u = 2\lambda - \xi$, and poles of order 1 at $u = \lambda - \xi$, $u = \xi$ and $u = 3\lambda \pm \xi$. Of these points, $u = \xi - \lambda$, $u = \lambda - \xi$, $u = \xi$ and $u = 2\lambda - \xi$ fall into the strip $-\frac{1}{2}\lambda < u < \frac{3}{2}\lambda$. The zeros and poles of β are unchanged, so the solution of Eq. (4.15) inside this strip is now

$$g(u) = \tan^2(\tfrac{5}{2}u - \tfrac{\pi}{4}) \tan[\tfrac{5}{2}(u+\xi)] \cot[\tfrac{5}{2}(u-\xi)]. \tag{6.3}$$

It immediately follows that $\lim_{x\to\pm\infty} g_1(x) = -1$.

6.3. Computation of the order-$1/N$ corrections

The computation of the order-$1/N$ corrections is very similar to that presented in Section 4.4. We need simply to replace $\hat{t}_1$ and $\hat{t}_2$ by their negatives on the left-hand sides of Eqs. (4.28) and (4.29), and hence in Eqs. (4.35), (4.36) and (4.38). This is necessary for our choice of the branches of the logarithms of $\hat{t}_1$ and $\hat{t}_2$ to be consistent with the parities of m_1 and m_2. Once this change is made, the whole of Section 4.4 from Eq. (4.17) to Eq. (4.42) holds for this boundary condition.

Instead of the expression (4.43), we now consider

$$\sum_{j=1}^{2} \int_{-\infty}^{\infty} \Big([\ln \hat{t}_j(x)]' \ln \hat{T}_j(x) - \ln[-\hat{t}_j(x)] [\ln \hat{T}_j(x)]' \Big) \, dx. \tag{6.4}$$

The left-hand side of Eq. (4.49) is unchanged, but using the limits

$$\hat{t}_1(\infty) = \hat{t}_2(\infty) = 2\cos\lambda, \qquad \hat{t}_1(-\infty) = -1, \qquad \hat{t}_2(-\infty) = 0, \tag{6.5}$$

the right-hand side is replaced by

$$\frac{1}{4\pi^2} \left[4L\Big(\frac{1}{2\cos\lambda}\Big) + 2L(1) \right] = \tfrac{11}{60}. \tag{6.6}$$

Hence in place of (4.50) we obtain

$$\ln l(u) = -\frac{2\pi}{N} \sin(5u) \left[-\tfrac{11}{120} + \tfrac{1}{4} \boldsymbol{mCm} + \sum_{j=1}^{2} \sum_{k=1}^{m_j} I_k^{(j)} \right]. \tag{6.7}$$

The minimal solution $m_1 = m_2 = 1$ of Eq. (6.1) gives $\boldsymbol{mCm} = 2$, so we have $\Delta = \frac{7}{16}$ and the identification

$$n + \tfrac{1}{2} = \tfrac{1}{4} \boldsymbol{mCm} + \sum_{j=1}^{2} \sum_{k=1}^{m_j} I_k^{(j)}. \tag{6.8}$$

Summing over the leading band of eigenvalues thus gives

$$Z_{N_0}(q) = q^{-\frac{c}{24} + \Delta_{2,1} - \frac{1}{2}} \sum_{\substack{m_1 \text{ odd} \\ m_2 \text{ odd}}} q^{\frac{1}{4}\boldsymbol{mCm}} \begin{bmatrix} m_1 + n_1 \\ m_1 \end{bmatrix} \begin{bmatrix} m_2 + n_2 \\ m_2 \end{bmatrix}. \tag{6.9}$$

Eliminating n_1 and n_2 using Eq. (6.1) and taking $N_0 \to \infty$ finally yields

$$Z(q) = q^{-\frac{c}{24} + \Delta_{2,1} - \frac{1}{2}} \sum_{\substack{m_1 \text{ odd} \\ m_2 \text{ odd}}} \frac{q^{\frac{1}{4}\boldsymbol{mCm}}}{(q)_{m_1}} \begin{bmatrix} \frac{1}{2}(m_1 + 1) \\ m_2 \end{bmatrix} = \chi_{2,1}(q). \tag{6.10}$$

7. The character $\chi_{2,2}$

7.1. Classification of zeros

Under the (2, 2) boundary condition we see, in addition to the usual four string types, both the "frozen" zeros of Section 5.1 and the zeros on the real u-axis of Section 6.1. Once again we see that these latter zeros become strings of type 2 for N sufficiently large.

As in Section 5.1, we let $\sigma = 1$ for contents with the frozen 1-string and $\sigma = -1$ otherwise. With the definitions of Eq. (4.3), we then observe the $(\boldsymbol{m}, \boldsymbol{n})$-system

$$m_1 + n_1 = \tfrac{1}{2}(N + m_2 + \sigma), \qquad m_2 + n_2 = \tfrac{1}{2}(m_1 - \sigma + 1), \tag{7.1}$$

so that m_1 is even and m_2 is odd. Using Eq. (7.1), the total number of eigenvalues is correctly computed to be

$$\sum_{\sigma} \sum_{\substack{m_1 \text{ even} \\ m_2 \text{ odd}}} \binom{m_1 + n_1 - \delta_{\sigma,1}}{m_1 - \delta_{\sigma,1}} \binom{m_2 + n_2}{m_2} = A^N_{2,2}. \tag{7.2}$$

7.2. Computation of the order-1/N corrections

With the same height $r = 2$, the free energies under this boundary condition are the same as those given in Section 6.2. We now proceed precisely in the manner of Section 5.2, with the simple replacement of $\hat{t}_1$ by $-\hat{t}_1$ and $-\hat{t}_2$ by $\hat{t}_2$ in accordance with the parities of m_1 and m_2. The calculation of Section 5.2 then applies from Eq. (5.3) to Eq. (5.7). The limits

$$\hat{t}_1(\infty) = \hat{t}_2(\infty) = 2\cos(3\lambda), \qquad \hat{t}_1(-\infty) = -1, \qquad \hat{t}_2(-\infty) = 0, \tag{7.3}$$

change the right-hand side of (5.9) to

$$-\frac{1}{4\pi^2}\left[4L\big(-2\cos(3\lambda)\big) - 2L(1)\right] = -\tfrac{1}{60}. \tag{7.4}$$

Hence we obtain

$$\ln l(u) = -\frac{2\pi}{N}\sin(5u)\left[\tfrac{1}{120} + \tfrac{1}{4}\boldsymbol{m}C\boldsymbol{m} - \tfrac{1}{2}(m_1 - m_2)\sigma + \sum_{j=1}^{2}\sum_{k=1}^{m_j} I_k^{(j)}\right]. \tag{7.5}$$

The minimal solution $m_1 = 0$ and $m_2 = 1$ with $\sigma = -1$ of Eq. (7.1) leads to the identifications $\Delta = \frac{3}{80}$ and

$$n = \tfrac{1}{4}\boldsymbol{m}C\boldsymbol{m} - \tfrac{1}{2}(m_1 - m_2)\sigma + \sum_{j=1}^{2}\sum_{k=1}^{m_j} I_k^{(j)}, \tag{7.6}$$

with $I^{(1)}_{m_1} = 0$ if $\sigma = 1$. Summing over the leading band of eigenvalues, we have

$$Z_{N_0}(q) = q^{-\frac{c}{24}+\Delta_{2,2}} \sum_{\sigma} \sum_{\substack{m_1 \text{ even} \\ m_2 \text{ odd}}} q^{\frac{1}{4}\boldsymbol{m}C\boldsymbol{m}-\frac{1}{2}(m_1-m_2)\sigma} \begin{bmatrix} m_1+n_1-\delta_{\sigma,1} \\ m_1-\delta_{\sigma,1} \end{bmatrix} \begin{bmatrix} m_2+n_2 \\ m_2 \end{bmatrix}. \tag{7.7}$$

Eliminating n_1 and n_2 using Eq. (7.1), and summing over σ using the recurrence (5.13), we obtain

$$Z_{N_0}(q) = q^{-\frac{c}{24}+\Delta_{2,2}} \sum_{\substack{m_1 \text{ odd} \\ m_2 \text{ odd}}} q^{\frac{1}{4}\boldsymbol{m}C\boldsymbol{m}-\frac{1}{2}m_1} \begin{bmatrix} \frac{1}{2}(N_0+m_2+1) \\ m_1 \end{bmatrix} \begin{bmatrix} \frac{1}{2}(m_1+1) \\ m_2 \end{bmatrix}. \tag{7.8}$$

Finally, taking $N_0 \to \infty$ gives

$$Z(q) = q^{-\frac{c}{24}+\Delta_{2,2}} \sum_{\substack{m_1 \text{ odd} \\ m_2 \text{ odd}}} \frac{q^{\frac{1}{4}\boldsymbol{m}C\boldsymbol{m}-\frac{1}{2}m_1}}{(q)_{m_1}} \begin{bmatrix} \frac{1}{2}(m_1+1) \\ m_2 \end{bmatrix} = \chi_{2,2}(q). \tag{7.9}$$

8. The character $\chi_{3,1}$

8.1. Classification of zeros

Under the (3, 1) boundary condition, the zero patterns of eigenvalues of $\boldsymbol{T}$ are very simple. We see the usual string types, no zeros on the real u-axis, and no "frozen" zeros. Defining $(\boldsymbol{m}, \boldsymbol{n})$ by Eq. (4.3) we then observe

$$m_1 + n_1 = \tfrac{1}{2}(N + m_2 + 1), \qquad m_2 + n_2 = \tfrac{1}{2}m_1, \tag{8.1}$$

so that m_1 is even and m_2 is odd. Using Eq. (8.1), the total number of eigenvalues is correctly computed to be

$$\sum_{\substack{m_1 \text{ even} \\ m_2 \text{ odd}}} \binom{m_1+n_1}{m_1} \binom{m_2+n_2}{m_2} = A^N_{3,1}. \tag{8.2}$$

8.2. Computation of the order-1/N corrections

As there are no zeros of $\boldsymbol{T}$ on the real u-axis, the order-1 analyticity of $\boldsymbol{t}$ is determined solely by the zeros and poles of the normalizing functions β and α. Since the function β is the same for all boundary conditions, the order-1 analyticity is as given in Section 4.3, but with the product $\alpha_3(u-\xi)\,\alpha_{-3}(u+\xi)$ now inducing zeros at $u = 2\lambda + \xi$ and $u = 4\lambda - \xi$, and poles at $u = \lambda + \xi$, $u = 3\lambda \pm \xi$ and $u = 5\lambda - \xi$. These additional zeros and poles all fall inside $\frac{3}{2}\lambda < u < \frac{9}{2}\lambda$, so the solution (4.16) for g inside the interval $-\frac{1}{2}\lambda < u < \frac{3}{2}\lambda$ is unchanged for the (3, 1) boundary condition.

Indeed, the differences between the computation of the order-$1/N$ corrections for the (3, 1) and the (1, 1) boundary conditions are also very small. All of the calculation from

Eq. (4.17) to Eq. (4.50) proceeds in an identical fashion, with the simple replacement of $\hat{t}_2$ by its negative in accordance with the change in parity of m_2.

The minimal solution of Eq. (8.1) is $m_1 = 2$ and $m_2 = 1$, so $\Delta = \frac{3}{2}$ and Eq. (4.51) is replaced by

$$n + \tfrac{3}{2} = \tfrac{1}{4}\boldsymbol{mCm} + \sum_{j=1}^{2} \sum_{k=1}^{m_j} I_k^{(j)}. \tag{8.3}$$

Summing over the leading band of eigenvalues, we therefore have

$$Z_{N_0}(q) = q^{-\frac{c}{24}} \sum_{\substack{m_1 \text{ even} \\ m_2 \text{ odd}}} q^{\frac{1}{4}\boldsymbol{mCm}} \begin{bmatrix} m_1 + n_1 \\ m_1 \end{bmatrix} \begin{bmatrix} m_2 + n_2 \\ m_2 \end{bmatrix}. \tag{8.4}$$

Eliminating n_1 and n_2 using Eq. (8.1), and taking $N_0 \to \infty$, we finally obtain the partition function

$$Z(q) = q^{-\frac{c}{24}} \sum_{\substack{m_1 \text{ even} \\ m_2 \text{ odd}}} \frac{q^{\frac{1}{4}\boldsymbol{mCm}}}{(q)_{m_1}} \begin{bmatrix} \frac{1}{2}m_1 \\ m_2 \end{bmatrix} = \chi_{3,1}(q). \tag{8.5}$$

9. The character $\chi_{3,2}$

9.1. Classification of zeros

For the (3,2) boundary condition we see the usual four strings, no zeros on the real u-axis, and the "frozen" 1-string of type 1 for certain string contents. As in Sections 5.1 and 7.1, we let $\sigma = 1$ for contents with the frozen 1-string and $\sigma = -1$ otherwise. With the definitions of Eq. (4.3), we then observe the $(\boldsymbol{m}, \boldsymbol{n})$-system

$$m_1 + n_1 = \tfrac{1}{2}(N + m_2 + \sigma + 1), \qquad m_2 + n_2 = \tfrac{1}{2}(m_1 - \sigma), \tag{9.1}$$

so that m_1 and m_2 are odd. Using Eq. (9.1), the total number of eigenvalues is correctly computed to be

$$\sum_{\sigma} \sum_{\substack{m_1 \text{ odd} \\ m_2 \text{ odd}}} \binom{m_1 + n_1 - \delta_{\sigma,1}}{m_1 - \delta_{\sigma,1}} \binom{m_2 + n_2}{m_2} = A_{3,2}^{N}. \tag{9.2}$$

9.2. Computation of the order-1/N corrections

Under the (3,2) boundary condition, the order-1 analyticity is the same as under the (3,1) boundary. Hence the function g is again given by Eq. (4.16). The order-$1/N$ calculation now proceeds exactly as in Section 5.2, with the replacement of $-\hat{t}_2$ by $\hat{t}_2$ in accordance with the change in parity of m_2.

With this single alteration, the computation of Section 5.2 holds from Eq. (5.3) to Eq. (5.10). However, the change in parity of m_2 means that the minimal solution to the $(\boldsymbol{m},\boldsymbol{n})$-system (9.1) is $m_1 = m_2 = 1$ with $\sigma = -1$. Hence $\Delta = \frac{3}{5}$ and the integer n of Eq. (3.3) is given by

$$n + \tfrac{1}{2} = \tfrac{1}{4}\boldsymbol{m}C\boldsymbol{m} - \tfrac{1}{2}(m_1 - m_2)\sigma + \sum_{j=1}^{2}\sum_{k=1}^{m_j} I_k^{(j)}. \tag{9.3}$$

Summing over all eigenvalues in the leading band then gives

$$Z_{N_0}(q) = q^{-\frac{c}{24}+\Delta_{3,2}-\frac{1}{2}} \sum_{\sigma} \sum_{\substack{m_1 \text{ odd} \\ m_2 \text{ odd}}} q^{\frac{1}{4}\boldsymbol{m}C\boldsymbol{m}-\frac{1}{2}(m_1-m_2)\sigma} \begin{bmatrix} m_1 + n_1 - \delta_{\sigma,1} \\ m_1 - \delta_{\sigma,1} \end{bmatrix} \begin{bmatrix} m_2 + n_2 \\ m_2 \end{bmatrix}. \tag{9.4}$$

Eliminating n_1 and n_2 using Eq. (9.1), and summing over σ using the recurrence (5.13), we obtain

$$Z_{N_0}(q) = q^{-\frac{c}{24}+\Delta_{3,2}-\frac{1}{2}} \sum_{\substack{m_1 \text{ even} \\ m_2 \text{ odd}}} q^{\frac{1}{4}\boldsymbol{m}C\boldsymbol{m}-\frac{1}{2}m_1} \begin{bmatrix} \frac{1}{2}(N_0 + m_2 + 2) \\ m_1 \end{bmatrix} \begin{bmatrix} \frac{1}{2}m_1 \\ m_2 \end{bmatrix}. \tag{9.5}$$

Finally, taking $N_0 \to \infty$ gives

$$Z(q) = q^{-\frac{c}{24}+\Delta_{3,2}-\frac{1}{2}} \sum_{\substack{m_1 \text{ even} \\ m_2 \text{ odd}}} \frac{q^{\frac{1}{4}\boldsymbol{m}C\boldsymbol{m}-\frac{1}{2}m_1}}{(q)_{m_1}} \begin{bmatrix} \frac{1}{2}m_1 \\ m_2 \end{bmatrix} = \chi_{3,2}(q). \tag{9.6}$$

10. Discussion

In this paper we have computed conformal partition functions of the tricritical hard square model with fixed boundaries by calculating analytically the order-$1/N$ corrections to all leading eigenvalues of the transfer matrix. Each partition function is found to be a single $c = \frac{7}{10}$ Virasoro character $\chi_{r,s}$, with r and s depending on the choice of boundary condition. This is in agreement with the results of Saleur and Bauer [18].

It is worthwhile noting that, as a bonus, the calculations of this paper also yield partition functions of the critical hard hexagon model [23]. This model has the same Boltzmann weights as tricritical hard squares, but with $u < 0$ in the ABF formulation. Once again, the heights 1 and 4 are identified with $\mu = 1$ and the heights 2 and 3 with $\mu = 0$. There are three degenerate ground states, which correspond to the complete filling ($\mu = 1$) of one of the sublattices A, B or C:

C A B C A B
A B C A B C
C A B C A B
A B C A B C

We denote by $Z_{P,Q}$ the conformal partition function of the model on a lattice with left boundary labelled by P and right boundary by Q. Generally, P and Q may correspond to sums of ground states.

By making the transformation $q \to 1/q$ in the finite partition functions Z_{N_0} and then taking $N_0 \to \infty$, we obtain $Z_{A,A} = \chi_{1,1} + \chi_{4,1} = b_0^0$, $Z_{A,B} = Z_{A,C} = \chi_{1,3} = b_2^0$, $Z_{A,B+C} = \chi_{2,1} + \chi_{3,1} = b_0^2$, and $Z_{A,A+B} = Z_{A,A+C} = \chi_{2,3} = b_1^1$. Here $\chi_{r,s}$ are now the $c = \frac{4}{5}$ Virasoro characters and b_m^l are the branching functions corresponding to the $\mathbb{Z}_3$ parafermion models. We note that for the $(2,1)$ and $(2,2)$ boundaries the classification of eigenvalues depends on the interpretation of zeros on the real u-axis. Hence in these cases the transformation is meaningless, since we have no description of the leading band of eigenvalues in the hard hexagon regime. The above results are in accordance with those of Refs. [31,18] for the three-state Potts model, which lies in the same universality class as the hard hexagon model.

Acknowledgements

This work is supported by the Australian Research Council. One of the authors (DO'B) is supported by his Dad.

Appendix A. The Rogers dilogarithm

In this appendix we briefly collect some results for the Rogers dilogarithm which enable us to evaluate the integrals that occur in our calculation. For details we refer the reader to, for example, Ref. [35]. The Rogers dilogarithm is defined for $0 < x < 1$ by

$$L(x) = -\tfrac{1}{2}\int_0^x \left(\frac{\ln(1-x)}{x} + \frac{\ln x}{1-x}\right) dx. \tag{A.1}$$

When $a > 0$, we can make the identification

$$\int_0^a \left(\frac{\ln(1+x)}{x} - \frac{\ln x}{1+x}\right) dx = 2L\left(\frac{a}{1+a}\right). \tag{A.2}$$

For our calculation we need the particular values

$$\begin{aligned} L(1) &= \tfrac{1}{6}\pi^2, \qquad L(\tfrac{1}{2}) = \tfrac{1}{12}\pi^2, \\ L\left(\frac{1}{2\cos\lambda}\right) &= L\big(-2\cos(3\lambda)\big) = \tfrac{1}{10}\pi^2, \end{aligned} \tag{A.3}$$

where $\lambda = \frac{1}{5}\pi$.

References

[1] A.A. Belavin, A.M. Polyakov and A.B. Zamolodchikov, Nucl. Phys. B 241 (1984) 333.
[2] J.L. Cardy, *in* Phase Transitions and Critical Phenomena, Vol. 11, ed. C. Domb and J.L. Lebowitz (Academic Press, London, 1987).
[3] H.J. de Vega and F. Woynarovich, Nucl. Phys. B 251 (1985) 439.
[4] F. Woynarovich and H.P. Eckle, J. Phys. A 20 (1987) L97.
[5] C.J. Hamer, G.R.W. Quispel and M.T. Batchelor, J. Phys. A 20 (1987) 5677.
[6] V.V. Bazhanov and N. Yu. Reshetikhin, Int. J. Mod. Phys. A 4 (1989) 115.
[7] A. Klümper, M.T. Batchelor and P.A. Pearce, J. Phys. A 24 (1991) 3111.
[8] P.A. Pearce and A. Klümper, Phys. Rev. Lett. 66 (1991) 974.
[9] A. Klümper and P.A. Pearce, J. Stat. Phys. 64 (1991) 13.
[10] A. Klümper and P.A. Pearce, Physica A 183 (1992) 304.
[11] A.E. Ferdinand and M.E. Fisher, Phys. Rev. 185 (1969) 832.
[12] A.I. Bugrij and V.N. Shadura, Phys. Lett. A 150 (1990) 171.
[13] G. Albertini, S. Dasmahapatra and B.M. McCoy, Int. J. Mod. Phys. A 7 Suppl. 1A (1992) 1.
[14] G. Albertini, S. Dasmahapatra and B.M. McCoy, Phys. Lett. A 170 (1992) 397.
[15] R. Kedem and B.M. McCoy, J. Stat. Phys. 71 (1993) 865.
[16] S. Dasmahapatra, R. Kedem, T.R. Klassen, B.M. McCoy and E. Melzer, Int. J. Mod. Phys. B 7 (1993) 3617.
[17] S. Dasmahapatra, R. Kedem, B.M. McCoy and E. Melzer, J. Stat. Phys. 74 (1994) 239.
[18] H. Saleur and M. Bauer, Nucl. Phys. B 320 (1989) 591.
[19] B. Nienhuis, *in* Phase Transitions and Critical Phenomena, Vol. 11, ed. C. Domb and J.L. Lebowitz (Academic Press, London, 1987).
[20] P. di Francesco, H. Saleur and J.B. Zuber, J. Stat. Phys. 49 (1987) 57.
[21] V. Pasquier, J. Phys. A 20 (1987) L1229.
[22] R.J. Baxter, J. Phys. A 13 (1980) L61.
[23] R.J. Baxter, Exactly Solved Models in Statistical Mechanics (Academic Press, London, 1982).
[24] R.J. Baxter and P.A. Pearce, J. Phys. A 16 (1983) 2239.
[25] D.A. Huse, Phys. Rev. Lett. 49 (1982) 1121.
[26] G.E. Andrews, R.J. Baxter and P.J. Forrester, J. Stat. Phys. 35 (1984) 193.
[27] I.V. Cherednik, Teor. Mat. Fiz. 61 (1984) 35.
[28] E.K. Sklyanin, J. Phys. A 21 (1988) 2375.
[29] R.E. Behrend, P.A. Pearce and D.L. O'Brien, J. Stat. Phys. 84 (1996) 1.
[30] H.W.J. Blöte, J.L. Cardy and M.P. Nightingale, Phys. Rev. Lett. 56 (1986) 742.
[31] J.L. Cardy, Nucl. Phys. B 324 (1989) 581.
[32] A. Berkovich, Nucl. Phys. B 431 (1994) 315.
[33] D.L. O'Brien and P.A. Pearce, J. Phys. A 30 (1997) 2353.
[34] R. Kedem, T.R. Klassen, B.M. McCoy and E. Melzer, Phys. Lett. B 307 (1993) 68.
[35] L. Lewin, Polylogarithms and Associated Functions (North-Holland, New York, 1981).